entropy

Article

# Cryptographic Algorithm Using Newton-Raphson Method and General Bischi-Naimzadah Duopoly System

**Abdelrahman Karawia**

Mathematics Department, Faculty of Science Mansoura University, Mansoura 35516, Egypt; abibka@mans.edu.eg

**Abstract:** Image encryption is an excellent method for the protection of image content. Most authors used the permutation-substitution model to encrypt/decrypt the image. Chaos-based image encryption methods are used in this model to shuffle the rows/columns and change the pixel values. In parallel, authors proposed permutation using non-chaotic methods and have displayed good results in comparison to chaos-based methods. In the current article, a new image encryption algorithm is designed using combination of Newton-Raphson's method (non-chaotic) and general Bischi-Naimzadah duopoly system as a hyperchaotic two-dimensional map. The plain image is first shuffled by using Newton-Raphson's method. Next, a secret matrix with the same size of the plain image is created using general Bischi-Naimzadah duopoly system. Finally, the XOR between the secret matrix and the shuffled image is calculated and then the cipher image is obtained. Several security experiments are executed to measure the efficiency of the proposed algorithm, such as key space analysis, correlation coefficients analysis, histogram analysis, entropy analysis, differential attacks analysis, key sensitivity analysis, robustness analysis, chosen plaintext attack analysis, computational analysis, and NIST statistical Tests. Compared to many recent algorithms, the proposed algorithm has good security efficiency.

**Keywords:** Newton-Raphson's method; chaos; image encryption/decryption; security analysis

check for updates

**Citation:** Karawia, A. Cryptographic Algorithm Using Newton-Raphson Method and General Bischi-Naimzadah Duopoly System. *Entropy* **2021**, *23*, 57. https://doi.org/10.3390/e23010057

Received: 7 November 2020
Accepted: 26 December 2020
Published: 31 December 2020

## 1. Introduction

Digital images play a critical role in the world today. Digital images make up 70% of the transmitted data via the Internet [1]. They often contain sensitive and valuable information which requires protection against unauthorised access in various applications such as military images, medical images and Satellite images. Therefore, researchers have been designing methods to protect digital images from piracy while they are transferred from one place to another such as encryption algorithms via chaos [2–6], DNA coding [7], and wavelets [8]. Also S-boxes play an excellent role in confirming the resistance of block ciphers against cryptanalysis [9]. In Reference [10], the authors presented an efficient algorithm based on a class of Mordell elliptic curves to generate S-boxes. One of the most stable and powerful public key cryptosystems has been proven to be the Elliptic Curve Cryptography, which is popular for its high performance. But improving protection by increasing the duration of the key is inefficient [11,12].

Among the many ways of image cryptography, the image cryptography based on chaotic map will selected over the past two decades. This is because the chaotic mappings have necessary proprieties such as high sensitivity to the initial conditions and the parameters, nonlinearity, non-periodicity, and pseudorandomness [13–17]. Numerous researchers have presented image cryptography algorithms via chaotic maps. Some of these algorithms have limited key space, weak keys, vulnerability to chosen plaintext/ciphertext attacks [18–20]. Almost all the authors used the permutation-substitution (confusion-diffusion) model to encrypt/decrypt the image. There are different permutation methods, from performing a shuffling to rows/columns to performing more complicated iterative processes. For example, in Reference [3], the authors proposed rows/columns shuffling algorithm using the logistic map to get permutation. Karawia in Reference [6] suggested an image encryption algorithm using Fisher-Yates shuffling to obtain permutation while Shakiba in Reference [21] performed cyclic shifts to the rows/columns via Chebyshev mapping to achieve permutation. Xiao et al. in Reference [22] used switch control mechanism to perform permutation for rows and columns of plain image. For substitution, majority of the authors applied the XOR processes [3–6,21,23], or addition modular 256 during the substitution stage of encryption [24]. There are many maps (chaotic and hyperchaotic) utilized to design encryption algorithms, for example, 1D chaotic map in Reference [25], 2D generalized Arnold map in Reference [26], 3D Cat chaotic map in Reference [27,28], and 4D chaotic map in Reference [29].

Many of the known chaotic image encryption algorithms are resistanceless for chosen plaintext attacks(CPA). These image encryption algorithms are broken by Li et al., algorithm [30], such as References [25,31,32]. To avoid this, the image encryption algorithm must be dependent on the plain image and randomized [21,33]. Based on the dimension of the chaotic map, most of 1D-chaotic maps have simple forms and simple chaotic orbits and can be guessed. So image encryption based on 1D chaotic maps are low secure [19,34]. On the contrary, the hyperchaotic maps have more complicated form and complicated chaotic performance which make expectation of their chaotic orbits is difficult [35].

In the current article, we design an image encryption algorithm that uses Newton-Raphson's method, to shuffle the rows/columns of the plain image, and the general Bischi-Naimzadah duopoly system, to diffuse the pixels of the shuffled image. The general Bischi-Naimzada is selected to solve three essential problems: (i) the randomness of the chaotic sequences, (ii) the space of the secret key, and (iii) improving the security compared with the algorithms in literature. The chaotic sequence generated from it is extremely random. Also, it has eight parameters and two initial values and thus increasing the secret key space for the image encryption algorithm. In this algorithm, the key mixing proportion factor $K$ is utilized to generate the secret key [36]. So, the proposed algorithm depends on the plain image and it can provide CPA-security. For more details about chaos based image encryption techniques, see Reference [37].

The main contributions of the current article are: (i) using a 2D chaotic map (the general Bischi-Naimzadah duopoly system) with a large positive Lyapunov exponent, wide and uniform distribution, (ii) Performing rows/columns shuffle for the plain image using pseudo-random sequence generation based on Newton-Raphson's method, (iii) performing pixel diffusion to the shuffled image, and (iv) offering CPA-security for our algorithm.

This article is prepared as follows. In Section 2, the general Bischi-Naimzadah duopoly system is presented. The proposed algorithm is introduced in Section 3. In Section 4, security experimental results and comparative analyses are given. Finally, conclusions are mentioned in Section 5.

## 2. General Bischi-Naimzadah Duopoly System (GBNDS)

The image encryption needs a sequences of random numbers to generate a good secret image. The current paper takes advantage of the effectiveness of the general Bischi-Naimzadah duopoly system to generate pseudorandom numbers. The general Bischi-Naimzada game is a market vying between two companies based on sales constraints with the aim of maximising profits. The general Bischi-Naimzadah duopoly system is mathematically defined as [38]:

$$\begin{aligned} q_1(t+1) &= q_1(t) + \nu_1 q_1(t)[(1-\mu_1)(a-2bq_1(t)-bq_2(t))-c_1] \\ q_2(t+1) &= q_2(t) + \nu_2 q_2(t)[(1-\mu_2)(a-2bq_2(t)-bq_1(t))-c_2], \end{aligned} \tag{1}$$

where

$q_i$: the output of company $i = 1,2$,
$a > 0$: constant price,
$b > 0$: the market price slope,
$c_i$: the marginal cost, $i = 1,2$,

$\mu_i > 0$: associated with the sales constraint, $i = 1, 2$,
$\nu_i > 0$: the adjustment speed of company $i = 1, 2$.

The chaotic behavior of system (1) is observed by the values of the parameters: $a = 11.25$, $b = 0.5, c_1 = 0.20, c_2 = 0.30, \mu_1 = 0.002, \mu_2 = 0.60, \nu_1 = 0.20, \nu_2 = 0.70$ and initial values $q_{10} = 0.10, q_{20} = 0.20$. Figure 1a displays the bifurcation diagram of system (1) regarding the parameter $\mu_1$. Lyapunov exponent of system (1) regarding the parameter $\mu_1$ is shown in Figure 1b. Figure 2 displays phase diagram of system (1). It presents four unconnected chaotic areas. Whereas the phase diagram of system (1) at $\mu_1 = 0.97$ is given in Figure 3 and it presents a chaotic attractor. The main advantages of the proposed coding scheme compared to other systems in the literature is that the chaotic coding sequence extracted from the **GBNDS** is extremely random. This is because this it contains many chaotic regions for different values of the parameters. The proposed system also shows a great positive feature, which is the emergence of a very wide range of chaos and complex dynamics with the parameter $\mu_1$ in which the system (1) shows very complex chaotic behavior [38]. Moreover, incorporating the effects of sales constraints into the form has the advantage of increasing the number of parameters in the form and thus expanding the secret key space for the cryptography process. Also, a stable coexistence of multiple chaotic attractions is observed in this case [38].

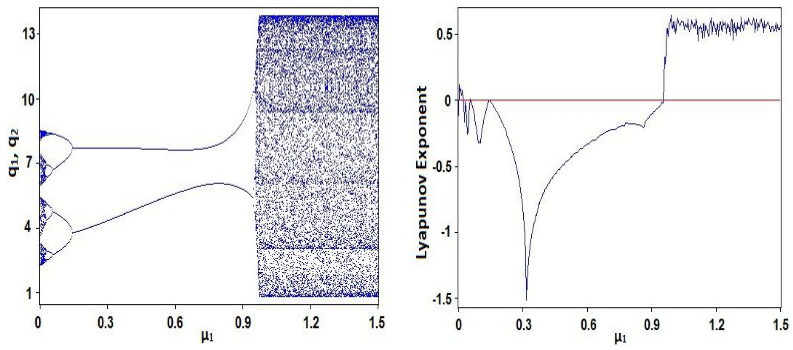

**Figure 1.** (**left**) Bifurcation diagram of system (1) regarding $\mu_1$, (**right**) Lyapunov exponent of system (1) regarding $\mu_1$.

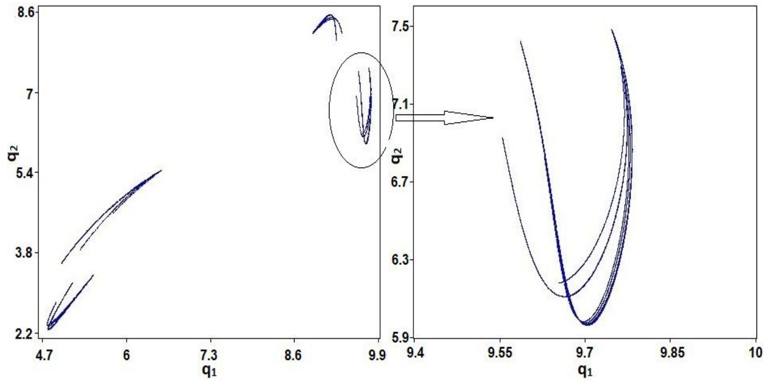

**Figure 2.** Phase diagram of system (1) for $a = 11.25, b = 0.5, c_1 = 0.20, c_2 = 0.30, \mu_1 = 0.002$, $\mu_2 = 0.60$, $\nu_1 = 0.20, \nu_2 = 0.70, q_{10} = 0.10$, and $q_{20} = 0.20$.

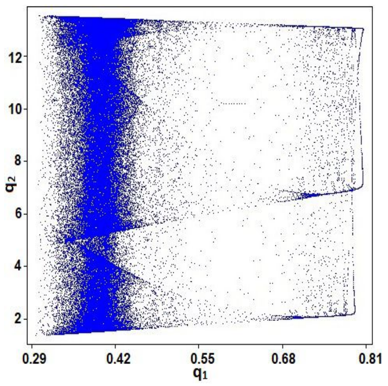

**Figure 3.** Phase diagram of system (1) for $a = 11.25, b = 0.5, c_1 = 0.20, c_2 = 0.30, \mu_1 = 0.97$, $\mu_2 = 0.60,\ \nu_1 = 0.20, \nu_2 = 0.70, q_{10} = 0.10$, and $q_{20} = 0.20$.

## 3. The Proposed Algorithm

The proposed method applies confusion-diffusion model to encrypt the plain image. Sequences are generated by the points, calculated by Newton-Raphson's method, on a polynomial function. Based on these sequences, the rows/columns of the plain image are shuffled (confusion phase). By applying *XOR* between the shuffled image and the generated values of the chaotic system (1), the diffusion stage modifies the pixel values. In the current section, the key generation, rows/columns Shuffling, and an image encryption/decryption algorithms are presented.

### 3.1. The Key Generation

Suppose that $\mathbf{O} = (o_{ij}), \quad i = 1, 2, ..., M$, and $j = 1, 2, ..., N$, is the plain image. The secret key is generated by using the key mixing proportion factor $K$ as follows [36]:

$$K_s = \frac{1}{256} mod \left( \sum_{i=[\frac{(s-1)M}{2}]+1}^{[\frac{sM}{2}]} \sum_{j=1}^{N} o_{ij}, 256 \right), \quad s = 1, 2, \tag{2}$$

and, the key values $\zeta_s$ is changed via the following formula:

$$\zeta_s \leftarrow \frac{(\zeta_s + K_s)}{2}, \quad s = 1, 2, \tag{3}$$

where $[x]$ denoted to the nearest integer and $\zeta_s$ denoted to $q_{s0},\ s = 1, 2$.

The key space of the proposed algorithm consists of the polynomial function with degree $k$ and limits of $[\alpha, \beta]$ for the Newton-Raphson's method, two initial values and eight parameters for *GBNDS*. Then, for the confusion phase, select two values, $\alpha, \beta$, and one polynomial function based on Newton-Raphson's method, and for diffusion phase, two initial values, $q_{10}, q_{20}$, and eight parameters $a, b, c_1, c_2, \mu_1, \mu_2, \nu_1, \nu_2$ for the System (1).

### 3.2. Rows/Columns Shuffling (Confusion Phase)

In this section, we design a technique for generating a random permutation of the integers $\{1, 2, \ldots, n\}$. Then, we shuffle the rows/columns of the plain image via the random permutation sequences.

Suppose a polynomial function of degree $s$, $p(x) = \sum_{i=1}^{s} a_i x^i$, where $a_s \neq 0$ and $s > 1$, is defined on the interval $[\alpha, \beta]$. Take $x_0 = (\alpha + \beta)/2$ and Newton-Raphson's method generates the sequence $\{x_i\}_{i=0}^{\infty}$ by the following formula:

$$x_i = x_{i-1} - \frac{p(x_{i-1})}{p'(x_{i-1})}, \quad p'(x_{i-1}) \neq 0 \quad \forall \quad i = 1, 2, 3, \ldots \tag{4}$$

Suppose, the Newton-Raphson's method generates the points $\{x_1, x_2, x_3, \ldots, x_n\}$. To get more randomness, instead of $p(x_i)$, the sequence is defined as the fraction part of $p(x_i)$. This sequence depends on the polynomial $p(x)$ and the interval $[\alpha, \beta]$.

The standard NIST SP800-22 test is used to assess the efficiency of the pseudorandom number generator(PRNG) of Newton-Raphson's method, and Table 1 gives the test results. In Table 1, the random number generator has passed all the tests. So, it has a good randomness.

**Table 1.** NIST statistical test for PRNG-Newton-Raphson's method.

| Statistical Test | PRNG | Result |
|---|---|---|
| Frequency monobit test | 100/100 | PASS |
| Block frequency test | 99/100 | PASS |
| Rank test | 99/100 | PASS |
| Runs test | 97/100 | PASS |
| Longest runs test | 99/100 | PASS |
| Cumulative sums test | 100/100 | PASS |
| Discrete Fourier transform | 100/100 | PASS |
| Random excursion test | 56/58 | PASS |
| Random excursion variant test | 57/58 | PASS |
| Universal test | 96/100 | PASS |
| Approximate entropy | 97/100 | PASS |
| Linear complexity test | 99/100 | PASS |
| Serial | 99/100 | PASS |
| Non Overlapping templates test | 97/100 | PASS |
| Overlapping templates test | 100/100 | PASS |

Algorithm 1 is proposed to generate a random permutation of the integers $\{1, 2, \ldots, n\}$ based on Newton-Raphson's method as follows:

**Algorithm 1** Random-Permutation algorithm

```
Input: Size of random numbers, $n$, the polynomial $p(x)$, $\alpha$, and $\beta$.
Output: $S$, the random permutation of the integers $\{1, 2, \ldots, n\}$.
Step 1: Set $S = 1$, $x_0 = (\alpha + \beta)/2$, $x = p(x_0) - fix(p(x_0))$
Step 2: For $i = 2$ to $n$, compute
            $S = [S \quad i]$
            $k = ceil(i * x)$
            $S([k \quad i]) = S([i \quad k])$
            $x_1 = x_0 - p(x_0)/p'(x_0)$
            $x = p(x_1) - fix(p(x_1))$
            $x_0 = x_1$
        End For
Step 3: $S$
```

Suppose the size of the plain image is $M \times N$. Algorithm 2 is designed to shuffle the plain image based on the random permutation sequences of Algorithm 1. It may be processed as in Algorithm 2.

### *3.3. Diffusion Phase*

The system (1) is utilized to generate a chaotic sequence of size $M \times N$. Then, reshape it to be of size $1 \times MN$, $Q = \{q_1, q_2, \ldots, q_{MN}\}$. The sequence $Q$ is modified using the following formula:

$$q_i = mod(ceil(q_i \times 10^{14}), 256), i = 1, 2, \ldots, MN. \tag{5}$$

**Algorithm 2** Row/Columns shuffling algorithm

```
Input: The plain image, $O$, the polynomial $p(x)$, $\alpha_1, \alpha_2, \beta_1$, and $\beta_2$.
Output: $H$, the shuffled image.
Step 1: Set $[M, N] = size(O)$
Step 2: Use Algorithm 1, with polynomial $p(x)$, and interval $[\alpha_1, \beta_1]$, to generate a random
        permutation of size $M$ for shuffling the rows, say $S_{Rows}$.
Step 3: Use Algorithm 1, with polynomial $p(x)$, and interval $[\alpha_2, \beta_2]$, to generate a random
        permutation of size $N$ for shuffling the columns, say $S_{Columns}$.
Step 4: For $i = 1$ to $M$, compute
            For $j = 1$ to $N$, compute
                $H(i,j) = O(S_{Rows}(i), S_{Columns}(j))$
            End For j
        End For i
Step 5: $H$, the shuffled image.
```

Moreover, the shuffled image $H$ is reshaped to be of size $1 \times MN$, $H = \{h_1, h_2, \ldots, h_{MN}\}$. Finally, $XOR$ is applied between each pixel in $H$ and corresponding chaotic value of $X$, $D = XOR(H, X)$ (diffusion phase). The algorithm of diffusion phase may be processed as follows:

**Algorithm 3** Diffusion algorithm

```
Input: The shuffled image, $H, q_{10}, q_{20}, a, b, c_1, c_2, \mu_1, \mu_2, \nu_1$, and $\nu_2$.
Output: $D$, the diffusion vector.
Step 1: Reshape $H$, $H = \{h_1, h_2, ..., h_{MN}\}$.
Step 2: Covert $H$ to binary, $H_b$.
Step 3: Set $q_1(0) = q_{10}, q_2(0) = q_{20}$.
Step 4: Perform initial iterations,
    For $t = 0$ to 999
        $q_1(t+1) = q_1(t) + \nu_1 q_1(t)[(1-\mu_1)(a - 2bq_1(t) - bq_2(t)) - c_1]$
        $q_2(t+1) = q_2(t) + \nu_2 q_2(t)[(1-\mu_2)(a - 2bq_2(t) - bq_1(t)) - c_2]$
    End For
Step 5: Set $q_1(0) = q_1(1000), q_2(0) = q_2(1000)$.
Step 6: For $t = 0$ to $MN - 1$
        $q_1(t+1) = q_1(t) + \nu_1 q_1(t)[(1-\mu_1)(a - 1(t) - bq_2(t)) - c_1]$
        $q_2(t+1) = q_2(t) + \nu_2 q_2(t)[(1-\mu_2)(a - 2bq_2(t) - bq_1(t)) - c_2]$
        $q(t+1) = (q_1(t+1) + q_2(t+1))/2$
    End For
Step 7: Preprocess the values of $Q = \{q(1), q(2), ..., q(MN)\}$ as follows:
    $q(t) = mod(ceil(q(t) * 10^{14}), 256), t = 1, 2, ..., MN$.
Step 8: Covert $Q$ to binary, $Q_b$.
Step 9: Perform $XOR$ between $H_b$ and $Q_b$, say $D = XOR(H_b, Q_b)$.
```

### 3.4. The Encryption/Decryption Algorithm

The encrypted image is produced from Algorithm 3 by reshape diffusion vector $D$ to be of size $M \times N$, say $E$. The whole image encryption algorithm may be processed as in the Algorithm 4.

The Algorithm 4 (Image Encryption based on General Bischi-Naimzadah Duopoly System) will be referred to as **IEGBNDS** algorithm. Indeed, **IEGBNDS** algorithm can be applied to encrypt the color images. We can decompose color images into three grayscale images of red, green and blue colors (R, G, B components). After that we can encrypt them into their corresponding cipher images by applying the proposed algorithm. Then by re-joining the three cipher images of the R, G, B components, the color cipher image can be obtained.

```
Algorithm 4 Image encryption algorithm
    Input: The plain image, $O$, the polynomial $p(x)$, $\alpha$, $\beta$, $q_{10}, q_{20}, a, b, c_1, c_2, \mu_1, \mu_2, \nu_1$, and $\nu_2$.
    Output: $E$, the encrypted image.
    Step 1: Read the plain image, $O$.
    Step 2: Generate the secret key by using the key mixing proportion factor.
    Step 3: Call Algorithm 2 to get the shuffled image $H$.
    Step 4: Call Algorithm 3 to get the diffusion vector $D$.
    Step 5: Covert $D$ to decimal, say $D_d$.
    Step 6: Change the dimension of $D_d$ to $M \times N$, say $E$.
    Step 7: $E$ is the encrypted image.
```

The decryption algorithm is the inverse steps of **IEGBNDS** algorithm. Figure 4 displays the block diagram of **IEGBNDS** algorithm.

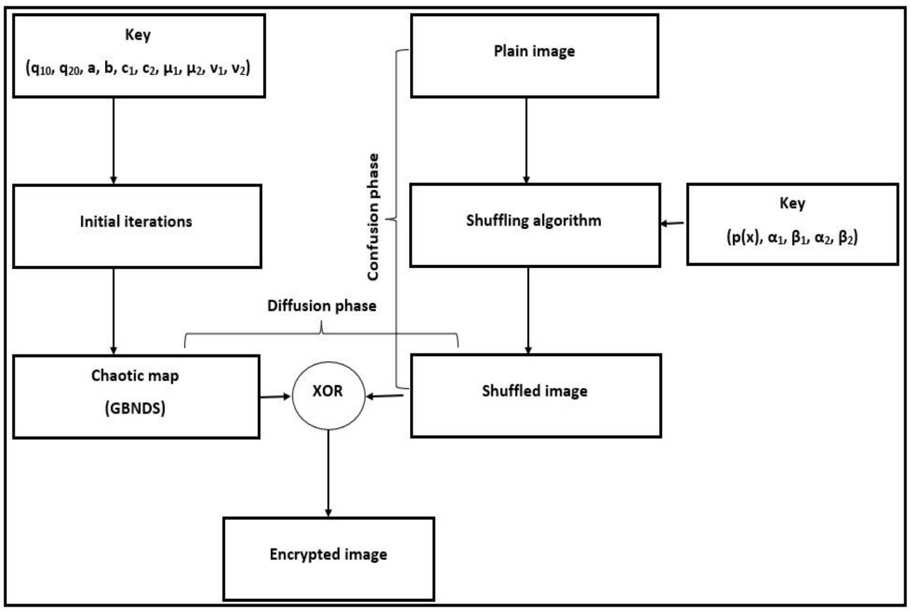

**Figure 4.** Block diagram of the proposed algorithm.

## 4. Experimental Results

The **IEGBNDS** algorithm has been applied to several 512 × 512 pixel gray-scale images and very promising results have been accomplished. All codes are accomplished on a Windows 10 Laptop with Intel(R) Core(TM) i7 2.40 GHz, CPU with 12 GB RAM using MATLAB R2016b.

### *4.1. Key Space Analysis*

The key space must be large enough to hold out against brute-force attack. It must be above the value $2^{100}$ [39]. The key space of the **IEGBNDS** algorithm consists of the polynomial function with degree $k$ and limits of $[\alpha, \beta]$ for the Newton-Raphson's method, two initial values and eight parameters for $GBNDS$. If the accuracy $10^{-14}$ has been used then it will be equal to $10^{14(k+1)} + 10^{168} (>> 2^{100})$. Table 2 gives the key space of the **IEGBNDS** algorithm compared to some recent algorithms in literature.

**Table 2.** Key space of the **IEGBNDS** algorithm compared to some recent algorithms in literature.

| **Algorithm** | **IEGBNDS Algorithm** | [5] | [23] | [40] |
|---|---|---|---|---|
| Key space | $(10^{14(k+1)} + 10^{168}) > 2^{605}$ | $10^{140} \approx 2^{466}$ | $>10^4 \times 2^{208}$ | $2^{256}$ |

### *4.2. Histogram Analysis*

In a good encryption algorithms, the distribution of the pixel intensity values within a cipher image should be as similar to the uniform distribution as possible. Figures 5 and 6 show that the histograms of the cipher image is very similar to the uniform distribution. As the $\chi^2$ statistical test is used to measure the nearness of produced histograms to the uniform histogram. The statistical $\chi^2$-value is evaluated by [6]:

$$\chi^2 = \sum_{i=1}^{256} \frac{(E_i - e_i)^2}{e_i}, \tag{6}$$

where the length of all possible values in an image is 256, $E_i$ is the observed event frequencies of $i - 1$ and $e_i$ is the expected event frequencies of $i - 1$, $i = 1, 2, ..., 256$. By evaluating the $\chi^2$-value with the level of significance $\alpha = 0.05$, we got $\chi_{0.05}(255) = 293.25$. So, Both distributions are nearly equal if $\chi^2(255) < 293.25$. Table 3 shows that all tested images are smaller than 293.25. Therefore, the cipher images histograms are close to the uniform distributions. In other words, an attacker cannot retrieve any valuable information from them.

(**a**) Lena

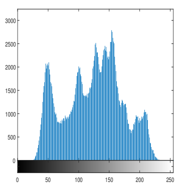
(**b**) Histogram of (**a**)

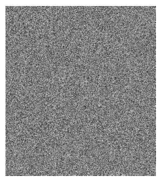
(**c**) Cipher image of (**a**)

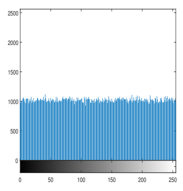
(**d**) Histogram of (**c**)

(**e**) Barbara

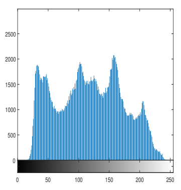
(**f**) Histogram of (**e**)

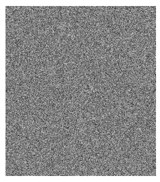
(**g**) Cipher image of (**e**)

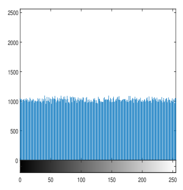
(**h**) Histogram of (**g**)

(**i**) Cameraman

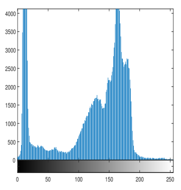
(**j**) Histogram of (**i**)

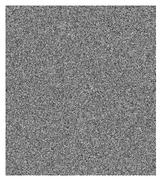
(**k**) Cipher image of (**i**)

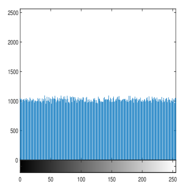
(**l**) Histogram of (**k**)

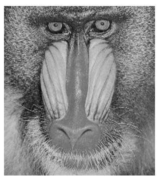
(**m**) Mandrill

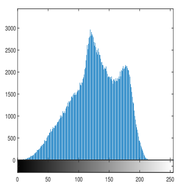
(**n**) Histogram of (**m**)

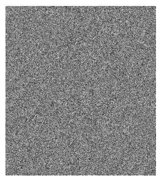
(**o**) Cipher image of (**m**)

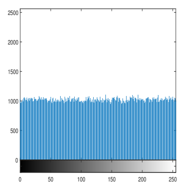
(**p**) Histogram of (**o**)

**Figure 5.** Plain images, cipher images and their corresponding histograms.

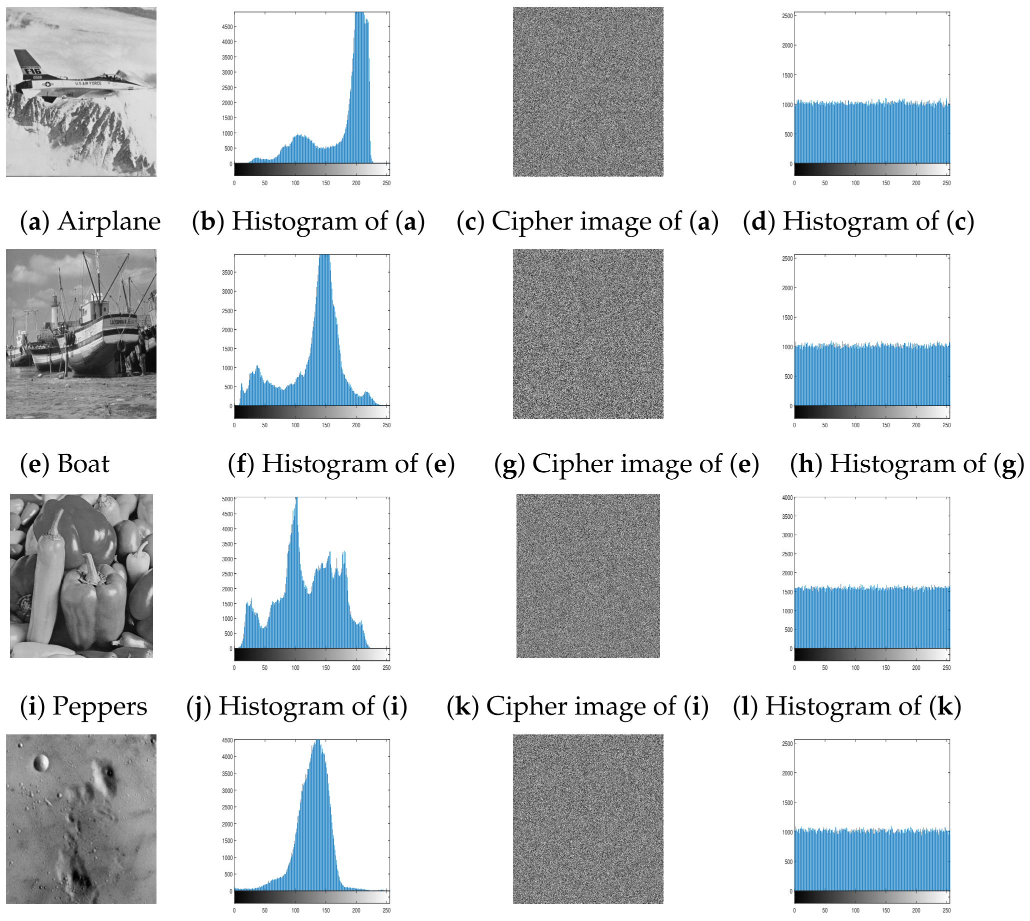

(**a**) Airplane (**b**) Histogram of (**a**) (**c**) Cipher image of (**a**) (**d**) Histogram of (**c**)

(**e**) Boat (**f**) Histogram of (**e**) (**g**) Cipher image of (**e**) (**h**) Histogram of (**g**)

(**i**) Peppers (**j**) Histogram of (**i**) (**k**) Cipher image of (**i**) (**l**) Histogram of (**k**)

(**m**) Moon_surface (**n**) Histogram of (**m**) (**o**) Cipher image of (**m**) (**p**) Histogram of (**o**)

**Figure 6.** Plain images, cipher images and their corresponding histograms.

**Table 3.** $\chi^2$-values of the histograms of the cipher images at $a = 11.25, b = 0.5, c_1 = 0.20, c_2 = 0.30,$ $\mu_1 = 0.002, \mu_2 = 0.60, \nu_1 = 0.20, \nu_2 = 0.70, q_{10} = 0.10$, and $q_{20} = 0.20$.

| Image | $\chi^2$-Value |
|---|---|
| Lena | 286.52 |
| Barbara | 256.74 |
| Cameraman | 252.88 |
| Mandrill | 275.24 |
| Airplane | 279.64 |
| Boat | 260.23 |
| Peppers | 288.74 |
| Moon_surface | 249.12 |

### Histogram Statistics

The variance and standard deviation are dispersion metrics applied in graphic histograms to help the effects of visual inspection. They calculate how often the elements of a dataset differ across the average with respect to each other. The same average value (mean) can be in two datasets, but the differences may be dramatically different. If the histogram has the lower variance then it has the more uniform of the graphic histogram, which is calculated by the following formula:

$$V = \frac{1}{256}\sum_{i=1}^{256}(\theta_i - \bar{\theta})^2, \tag{7}$$

where

$$\bar{\theta} = \frac{M \times N}{256}, \tag{8}$$

$\theta_i$ is the frequency for each pixel's value from $0 - 255$ of the histogram, $i = 1, 2, \ldots, 256$, $\bar{\theta}$ is the histogram mean.

The standard deviation helps us to know the arithmetic average of the dataset's variations relative to the mean. It is calculated as follows:

$$S = \sqrt{V}, \tag{9}$$

where $V$ is the histogram variance.

Table 4 presents the histogram statistics for the plain and cipher images of the tested images for the **IEGBNDS** algorithm and the encryption algorithm in Reference [41].

**Table 4.** Histogram statistics for the **IEGBNDS** algorithm and the encryption algorithm in Reference [41].

| Image | Plain Image | | Cipher Image | | | |
|---|---|---|---|---|---|---|
| | | | IEGBNDS | | [41] | |
| | V | S | V | S | V | S |
| lena ($256 \times 256$) | 38451 | 196.1 | 396 | 19.9 | 414 | 20.3 |
| lena ($512 \times 512$) | 633397 | 795.9 | 3171 | 56.3 | 3340 | 57.8 |

### *4.3. Entropy Analysis*

Information entropy [7] is utilized to detect the randomness of the cipher image. It is computed as follows:

$$H = \sum_{i=0}^{255} P_i log_2(\frac{1}{P_i}), \tag{10}$$

where $P_i$ is the probability associated with gray level $i$. The largest value of the entropy reflects the randomness of the encrypted image. The maximum value of the entropy in our case is 8. Table 5 gives the information entropy for the plain and cipher images of the tested images. All values of entropy based on our algorithm are close to 8. In addition, the **IEGBNDS** algorithm gives average better than most averages of the listed recent algorithms. Based on the results of entropy, the **IEGBNDS** algorithm has reasonable protection.

**Table 5.** Information entropy analysis of the **IEGBNDS** algorithm compared to some recent algorithms in literature.

| Image | Information Entropy | |
|---|---|---|
| | Plain Image | Encrypted Image |
| Lena | 7.4475 | 7.9992 |
| Barbara | 7.6338 | 7.9993 |
| Cameraman | 7.0518 | 7.9993 |
| Mandrill | 7.2933 | 7.9992 |
| Airplane | 6.6823 | 7.9992 |
| Boat | 7.2151 | 7.9993 |
| Peppers | 7.4849 | 7.9992 |
| Moon_surface | 6.6974 | 7.9993 |
| Average | 7.1883 | 7.99925 |
| [5] (Average) | – | 7.99867 |
| [23] (Average) | – | 7.90252 |
| [40] (Average) | 7.266297 | 7.999224 |

### *4.4. Correlation Coefficients Analysis*

In the plain image, adjacent pixels have strong relationships. So, reducing these relationships is required to hold out against statistical attacks. The correlation coefficient between two adjacent pixels, $\theta$ and $\phi$, is defined as [6]:

$$r_{\theta\phi} = \frac{Cov(\theta, \phi)}{\sqrt(D(\theta)D(\phi))}, \tag{11}$$

where

$$Cov(\theta, \phi) = \frac{1}{N} \sum_{m=1}^{N} (\theta_m - E(\theta))(\phi_m - E(\phi)), \tag{12}$$

$$E(\theta) = \frac{1}{N} \sum_{m=1}^{N} \theta_m, \tag{13}$$

and

$$D(\theta) = \frac{1}{N} \sum_{m=1}^{N} (\theta_m - E(\theta))^2, \tag{14}$$

where $\theta$ and $\phi$ are selected randomly. 3000 pairs of adjacent pixels are chosen randomly from the plain and cipher images. Figure 7 displays the pixel intensity value's distribution of 3000 pairs for the Barbara image and its encrypted image in the three directions, diagonal, horizontal, and vertical. The correlation coefficients of the three directions for the **IEGBNDS** algorithm compared to some recent encryption algorithms based on the average of the correlation coefficients are given in Table 6. Table 6 shows that the **IEGBNDS** algorithm outperforms all of them at least in one direction. Also all values of $r_{\theta\phi}$ for the cipher images are close to zero. So, it can protect the image information.

**Table 6.** Correlation coefficient of the cipher images based on the **IEGBNDS** algorithm compared to some recent encryption algorithms in literature.

| **Image** | **Correlation Coefficient** | | |
|---|---|---|---|
| | **Horizontal** | **Vertical** | **Diagonal** |
| Lena | 0.0011 | −0.0026 | −0.0015 |
| Barbara | −0.0006 | −0.0015 | −0.0010 |
| Cameraman | −0.0035 | −0.0029 | −0.0015 |
| Mandrill | −0.0002 | −0.0005 | −0.0026 |
| Airplane | 0.0029 | −0.0020 | −0.0049 |
| Boat | −0.0034 | −0.0019 | 0.0010 |
| Peppers | −0.0035 | 0.0032 | 0.0017 |
| Moon_surface | −0.0013 | 0.0000 | 0.0011 |
| Average | 0.002063 | 0.001825 | 0.001913 |
| [5] (Average) | 0.007067 | 0.007867 | 0.014567 |
| [23] (Average) | 0.001544 | 0.001772 | 0.002678 |
| [40] (Average) | 0.003134 | 0.006602 | 0.004525 |

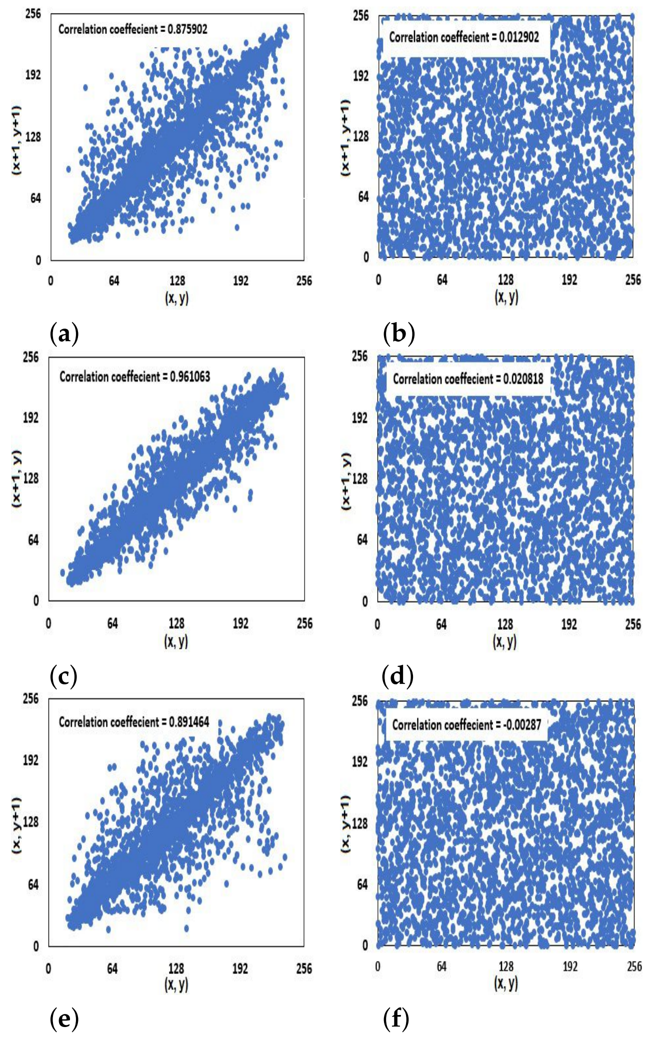

**Figure 7.** Distribution of adjacent pixels in the plain image (**a**,**c**,**e**) and the cipher image (**b**,**d**,**f**) for Barbara image in the three directions, diagonal, horizontal, and vertical.

## *4.5. Differential Attack Analysis*

The protection against differential attacks is required for any image encryption algorithm. There are two main measurements, (1) $NPCR$ (Number of Pixel Change Rate), and (2) $UACI$ (Unified Average Changing Intensity). These measurements evaluated the amount of differences between two images, and can be defined as [5]:

$$NPCR = \frac{\sum_{m,n} D(m,n)}{M \times N} \times 100\%, \tag{15}$$

$$UACI = \frac{1}{M \times N}\left[\sum_{m,n} \frac{|O(m,n) - E(m,n)|}{255}\right] \times 100\%, \tag{16}$$

where

$$D(m,n) = \begin{cases} 0 & \text{if } O(m,n) = E(m,n), \\ 1 & \text{otherwise.} \end{cases} \tag{17}$$

A single pixel of the plain image is selected randomly and it modified to $255 - v$, where $v$ is the original intensity value of pixel. The same key is utilized to encrypt the modified image and the plain image. Then, $NPCR$, and $UACI$ are calculated using the two cipher images. Table 7 shows $NPCR$ and $UACI$ for the tested images and compared them to some recent algorithms in literature. The **IEGBNDS** algorithm offers a good level of security. Based on the averages of $NPCR$ and $UACI$, the **IEGBNDS** algorithm outperforms all of them at least in one of the two measures. So, the **IEGBNDS** algorithm can be useful against differential attacks.

**Table 7.** NPCR and UACI of the tested images using the **IEGBNDS** algorithm and the recent algorithms.

| **Image** | **NPCR (%)** | **UACI%** |
|---|---|---|
| Ideal value [23] | 99.6094 | 33.4635 |
| Lena | 99.6326 | 33.4584 |
| Barbara | 99.6082 | 33.5339 |
| Cameraman | 99.6044 | 33.5797 |
| Mandrill | 99.6204 | 33.4392 |
| Airplane | 99.5907 | 33.4608 |
| Boat | 99.6086 | 33.4599 |
| Peppers | 99.6033 | 33.4868 |
| Moon_surface | 99.5998 | 33.4590 |
| **Average** | 99.6085 | 33.48471 |
| [5] (Average) | 99.6067 | 33.4267 |
| [23] (Average) | 99.6083 | 33.4521 |
| [40] (Average) | 99.6060 | 33.4646 |

## 4.6. Key Sensitivity Analysis

The sensitivity to the secret key is one of the important features of an excellent encryption algorithm. During the restoring plain image (decryption process), small changes in one of the initial values or parameter are made and we will observe the restoring image via the modified secret key. Table 8 shows the restoring images using the true secret key and the modified secret keys. The plain image cannot be restored by any of modified secret keys. Therefore, the **IEGBNDS** algorithm is highly sensitive to any changes of the secret key.

**Table 8.** The result of key sensitivity analysis.

| Cipher image | Decrypted with true key | Decrypted with wrong key $q_1(1) \times 10^{-14}$ | Decrypted with wrong key $q_2(1) \times 10^{-14}$ |
|---|---|---|---|
| 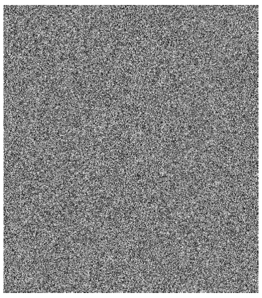 | 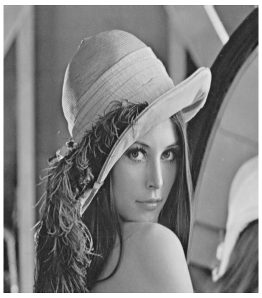 | 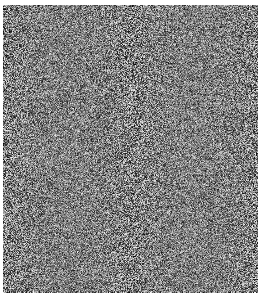 | 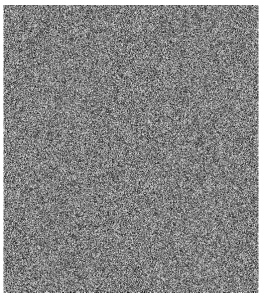 |
| Decrypted with wrong key $a \times 10^{-14}$ | Decrypted with wrong key $b \times 10^{-14}$ | Decrypted with wrong key $\mu_1 \times 10^{-14}$ | Decrypted with wrong key $\nu_1 \times 10^{-14}$ |
| 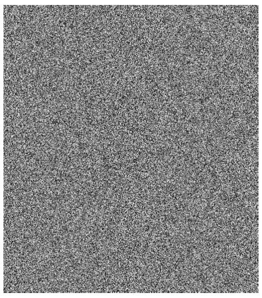 | 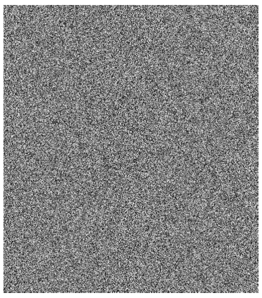 | 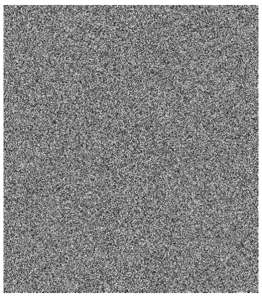 | 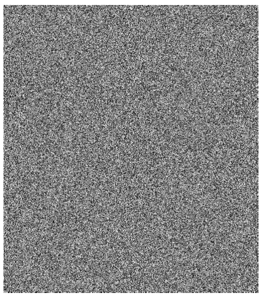 |

### *4.7. Robustness Analysis*

In real life, noise or data loss is occurred and the **IEGBNDS** algorithm is tested against these problems. Salt&Pepper noise with different densities are added to the cipher image of lena with size 512 × 512. Table 9 shows the decrypted images of the noisy encrypted images. Moreover, the decryption image of the encryption image with some data loss is shown in Table 9. Based on the result of Table 9, The **IEGBNDS** algorithm can be robust against the noise and data loss attacks.

**Table 9.** Robustness analysis of the **IEGBNDS** algorithm for lena image with size 512 × 512.

| Encrypted with salt&pepper(0.01) | Decryption of previous image | Encrypted with salt&pepper(0.05) | Decryption of previous image |
|---|---|---|---|
| 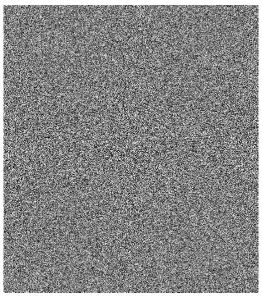 | 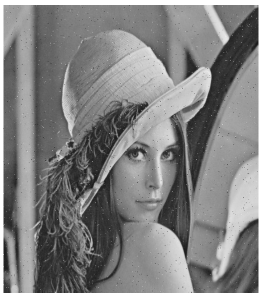 | 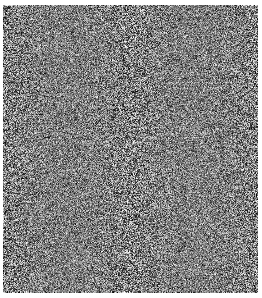 | 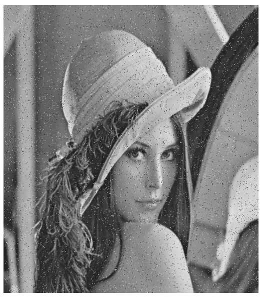 |
| Encrypted with salt&pepper(0.1) | Decryption of previous image | Encrypted with corp of 200 × 200 | Decryption of previous image |
| 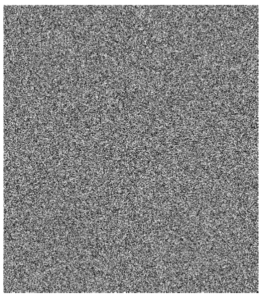 | 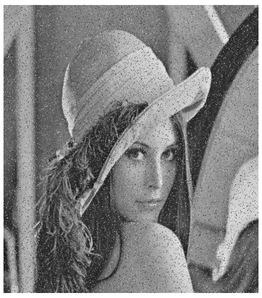 | 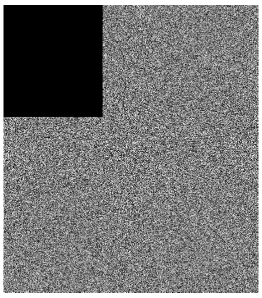 | 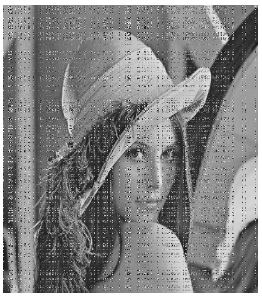 |

### *4.8. Chosen Plaintext Attack Analysis*

The **IEGBNDS** algorithm is sensitive to the key generation, $K_s$, in Equation (2) and different sequences will be generated by small changes in the plain image. So, the **IEGBNDS** algorithm can hold out against the plaintext attacks. Now, we will examine the **IEGBNDS** algorithm against the chosen plaintext attack. Suppose the attacker has the encrypted image and the running of the **IEGBNDS** algorithm for a short time. The algorithm of Reference [42] will be used to examine our algorithm against chosen plaintext attack. In this algorithm, the following notations will be used:

$P$: plain image,
$E$: encrypted image of $P$,
$D$: designed image, where $d_{mn} = 0, \quad m = 1, 2, \ldots, M, \quad n = 1, 2, \ldots, N,$
$E_D$: encrypted image of $D$,
$D_E$: decrypted image of $E$.

The *XOR* operations between the pixels of $E$ and $E_D$ are performed to obtain the plain image $P$. Based on the result of Figure 8, the decrypted image is totally unlike the plain image. Therefore, the **IEGBNDS** algorithm can resist chosen plaintext attack.

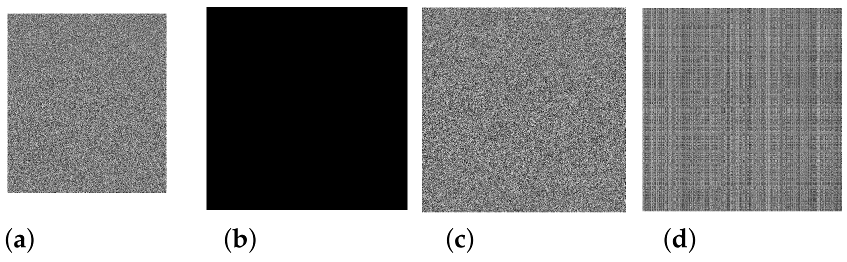

**Figure 8.** Analysis of chosen plaintext attack: (**a**) Encrypted image $E$, (**b**) designed image $D$, (**c**) encrypted image of $D$, (**d**) Decrypted image $D_E$.

### *4.9. Computational Analysis*

The average times of encryption and decryption algorithm for one hundred time are 34.11 ms and 30.57 ms (Tested image of size $512 \times 512$), respectively. On the other hand, for the tested image of size $M \times N$, the encryption algorithm needs $5\,MN + M + N + 2000$ operations. The complexity time for the decryption algorithm is equal to the complexity time of the encryption algorithm. Table 10 shows that the running time of the **IEGBNDS** algorithm is effective compared to some recent image encryption algorithms such as in Reference [40] by Shakiba and Reference [23] by Cao et al.

**Table 10.** Running time of the encryption for the **IEGBNDS** algorithm and the recent algorithms.

| Algorithm | Image Size | Running Time (ms) |
|---|---|---|
| **IEGBNDS** | $512 \times 512$ | 34.11 |
| [40] | $512 \times 512$ | $976 \pm 24.6$ |
| [23] | $256 \times 256$ | 32.43 |

### *4.10. NIST Statistical Tests*

NIST were established to test the randomness of generating cipher images created by encryption algorithms [43]. For the **IEGBNDS** algorithm, it is used to check the randomness of a sequence that consists of 100 cipher images of length $512 \times 512 \times 8 = 2{,}097{,}152$ bits. They were generated by using different random secret keys. Table 11 presents the results for 15 tests and all of them passed these tests.

**Table 11.** NIST statistical test for 100 cipher images by the **IEGBNDS** algorithm.

| Statistical Test | IEGBNDS Algorithm | Result |
|---|---|---|
| Frequency monobit test | 100/100 | PASS |
| Block frequency test | 99/100 | PASS |
| Rank test | 99/100 | PASS |
| Runs test | 99/100 | PASS |
| Longest runs test | 100/100 | PASS |
| Cumulative sums test | 99/100 | PASS |
| Discrete Fourier transform | 98/100 | PASS |
| Random excursion test | 56/58 | PASS |
| Random excursion variant test | 57/58 | PASS |
| Universal test | 99/100 | PASS |
| Approximate entropy | 98/100 | PASS |
| Linear complexity test | 100/100 | PASS |
| Serial | 100/100 | PASS |
| Non Overlapping templates test | 99/100 | PASS |
| Overlapping templates test | 100/100 | PASS |

## 5. Conclusions

In this article, the **IEGBNDS** algorithm via Newton-Raphson's method and general Bischi-Naimzadah duopoly system (**GBNDS**) has been suggested. Newton-Raphson's method has been used for shuffling the rows/columns of the plain image. **GBNDS** has been used to producing chaotic sequences to diffusion phase of image encryption algorithm. The extracted chaotic sequences from the **GBNDS** is extremely random based on the NIST statistical tests. Many security experiments are applied to evaluate the efficiency of our algorithm. The **IEGBNDS** algorithm has a large key space $(10^{14(k+1)} + 10^{168}(>>2^{100})$, the histograms of the generated cipher images are close to the uniform distributions, all entropy values for the cipher images based on **IEGBNDS** algorithm are close to 8, all correlation coefficient values for the cipher images are close to zero. The **IEGBNDS** algorithm outperforms some recent algorithms at least in one of the two measures, highly sensitive to small changes of the secret key, can be robust against the noise and data loss attacks, and can hold out against the plaintext attacks. In comparison to several recent algorithms, the **IEGBNDS** algorithm has a small running time. NIST statistical tests for 100 cipher images by the **IEGBNDS** algorithm are performed and all tests are passed. Finally, quantum image encryption algorithm based on **GBNDS** will be designed in the future to increase the security of the current algorithm.

**Funding:** This research received no external funding.

**Institutional Review Board Statement:** Not applicable.

**Informed Consent Statement:** Not applicable.

**Data Availability Statement:** Data sharing not applicable.

**Acknowledgments:** I deeply thank Shehzad Ahmed for his proof reading the paper.

**Conflicts of Interest:** The author declares no conflict of interest.

## References

1. Arab, A.; Rostami, M.; Ghavami, B. An image encryption method based on chaos system and AES algorithm. *J. Supercomput.* **2019**, *75*, 6663–6682. [CrossRef]
2. Yin, Q.; Wang, C. A new chaotic image encryption scheme using breadth-first search and dynamic diffusion. *Int. J. Bifurc. Chaos* **2018**, *28*, 1850047. [CrossRef]
3. Askar, S.; Karawia, A.; Alammar, F. Cryptographic algorithm based on pixel shuffling and dynamical chaotic economic map. *IET Image Process* **2018**, *12*, 158–167. [CrossRef]
4. Karawia, A. Encryption Algorithm of Multiple-Image Using Mixed Image Elements and Two Dimensional Chaotic Economic Map. *Entropy* **2018**, *20*, 801. [CrossRef]
5. Askar, S.; Karawia, A.; Al-Khedhairi, A.; Alammar, F. An Algorithm of Image Encryption Using Logistic and Two-Dimensional Chaotic Economic Maps. *Entropy* **2019**, *1*, 44. [CrossRef]
6. Karawia, A. Image encryption based on Fisher-Yates shuffling and three dimensional chaotic economic map. *IET Image Process* **2019**, *13*, 2086–2097. [CrossRef]
7. Wu, X.; Wang, K.; Wang, X.; Kan, H. Lossless chaotic color image cryptosystem based on DNA encryption and entropy. *Nonlinear Dynam.* **2017**, *90*, 855–875. [CrossRef]
8. Wu, X.; Wang, D.; Kurths, J.; Kan, H. A novel lossless color image encryption scheme using 2d dwt and 6d hyperchaotic system. *Inf. Sci.* **2016**, *349*, 137–153. [CrossRef]
9. Ivanov, G.; Nikolov, N.; Nikova, S. Cryptographically strong S-boxes generated by modified immune algorithm. In Proceedings of the International Conference on Cryptography and Information Security in the Balkans, Koper, Slovenia, 3–4 September 2015; pp. 31–42.
10. Azam, N.; Hayat, U.; Ikram, U. Efficient construction of a substitution box based on a Mordell elliptic curve over a finite field. *Front. Inform. Technol. El* **2019**, *20*, 1378–1389. [CrossRef]
11. Jia, N.; Liu, S.; Ding, Q.; Wu, S.; Pan, X. A New Method of Encryption Algorithm Based on Chaos and ECC. *J. Inf. Hiding Multimed. Signal Process.* **2016**, *7*, 637–643.
12. Hayat, U.; Azam, N. A novel image encryption scheme based on an elliptic curve. *Signal Process.* **2019**, *155*, 391–402. [CrossRef]
13. Tonga, X.; Zhanga, M.; Wang, Z.; Liu, Y.; Ma, J. An image encryption scheme based on a new hyperchaotic finance system. *Optik* **2015**, *126*, 2445–2452. [CrossRef]
14. Guo, H.; Zhang, X.; Zhao, X.; Yu, H.; Zhang, L. Quadratic function chaotic system and its application on digital image encryption. *IEEE Access* **2020**, *8*, 55540–55549. [CrossRef]

15. Pareschi, F.; Setti, G.; Rovatti, R. Implementation and testing of high-speed cmos true random number generators based on chaotic systems. *IEEE Trans. Circuits-I* **2010**, *57*, 3124–3137. [CrossRef]
16. Seyedzadeh, S.M.; Norouzi, B.; Mosavi, M.R.; Mirzakuchaki, S. A novel color image encryption algorithm based on spatial permutation and quantum chaotic map. *Nonlinear Dynam.* **2015**, *81*, 511–529. [CrossRef]
17. Wu, Y.; Hua, Z.; Zhou, Y. N-dimensional discrete cat map generation using laplace expansions. *IEEE Trans. Cybern.* **2016**, *46*, 2622–2633. [CrossRef]
18. Lian, S.; Sun, J.; Wang, Z. Security analysis of a chaos-based image encryption algorithm. *Phys. A* **2005**, *351*, 645–661. [CrossRef]
19. Skrobek, A. Cryptanalysis of chaotic stream cipher. *Phys. Lett. A* **2007**, *363*, 84–90. [CrossRef]
20. Yang, T.; Yang, L.; Yang, C. Cryptanalyzing chaotic secure communications using return maps. *Phys. Lett. A* **1998**, *245*, 495–510. [CrossRef]
21. Shakiba, A. A randomized CPA-secure asymmetric-key chaotic color image encryption scheme based on the Chebyshev mappings and one-time pad. *J. King Saud Univ. Comput. Inf. Sci.* **2019**. [CrossRef]
22. Xiao, S.; Yu, Z.; Deng, Y. Design and analysis of a novel chaos-based image encryption algorithm via switch control mechanism. *Secur. Commun. Netw.* **2020**, *2020*. [CrossRef]
23. Cao, C.; Sun, K.; Liu, W. A novel bit-level image encryption algorithm based on 2d-LICM hyperchaotic map. *Signal Process.* **2018**, *143*, 122–133. [CrossRef]
24. Shakiba, A. A novel randomized one-dimensional chaotic chebyshev mapping for chosen plaintext attack secure image encryption with a novel chaotic breadth first traversal. *Multimed. Tools Appl.* **2019**, *78*, 34773–34799. [CrossRef]
25. Pak, C.; Huang, L. A new color image encryption using combination of the 1d chaotic map. *Signal Process.* **2017**, *138*, 129–137. [CrossRef]
26. Rajendran, R.; Manivannan, D. A secure image cryptosystem using 2D arnold cat map and logistic map. *Int. J. Pharm. Technol.* **2016**, *8*, 25173–25182.
27. Gu, G.; Ling, J. A fast image encryption method by using chaotic 3D cat maps. *Optik* **2014**, *125*, 4700–4705. [CrossRef]
28. Mohamed, N.; El-Azeim, M.; Zaghloul, A. Improving Image Encryption Using 3D Cat Map and Turing Machine. *Int. J. Adv. Comput. Sci. Appl.* **2016**, *7*, 208–215.
29. Zhao, Y.; Gao, C.; Liu, J.; Dong, S. A Self-perturbed Pseudo-random Sequence Generator Based on Hyperchaos. *Chaos Soliton Fract. X* **2019**, *4*, 100023. [CrossRef]
30. Li, C.; Chen, M.; Lo, K. Breaking an image encryption algorithm based on chaos. *Int. J. Bifurcat. Chaos* **2011**, *21*, 3518–3524. [CrossRef]
31. Wang, X.; Teng, L.; Qin, X. A novel colour image encryption algorithm based on chaos. *Signal Process.* **2012**, *92*, 1101–1108. [CrossRef]
32. Li, Z.; Peng, C.; Li, L.; Zhu, X. A novel plaintext-related image encryption scheme using hyper-chaotic system. *Nonlinear Dynam.* **2018**, *94*, 1319–1333. [CrossRef]
33. Lindell, Y.; Katz, J. *Introduction to Modern Cryptography*; CRC Press: Boca Raton, FL, USA, 2014.
34. Li, C.; Zhang, L.; Ou, R.; Wong, K.; Shu, S. Breaking a novel colour image encryption algorithm based on chaos. *Nonlinear Dynam.* **2012**, *70*, 2383–2388. [CrossRef]
35. Ding, L.; Ding, Q. A Novel Image Encryption Scheme Based on 2D Fractional Chaotic Map, DWT and 4D Hyper-chaos. *Electronics* **2020**, *9*, 1280. [CrossRef]
36. Enzeng, D.; Zengqiang, C.; Zhuzhi, Y.; Zaiping, C. A chaotic images encryption algorithm with the key mixing proportion factor. In Proceedings of the 2008 International Conference on Information Management, Innovation Management and Industrial Engineering, Taipei, Taiwan, 19–21 December 2008; pp. 169–174.
37. Hosny, K. Multimedia Security Using Chaotic Maps: Principles and Methodologies. In *Studies in Computational Intelligence*; Springer: Berlin/Heidelberg, Germany, 2020.
38. Askar, S.; Al-Khedhairi, A. Local and Global Dynamics of a Constraint Profit Maximization for Bischi-Naimzada Competition Duopoly Game. *Mathematics* **2020**, *8*, 1458. [CrossRef]
39. Zhang, L.; Li, C.; Wong, K.; Shu, S.; Chen, G. Cryptanalyzing a chaos-based image encryption algorithm using alternate structure. *J. Syst. Softw.* **2012**, *85*, 2077–2085. [CrossRef]
40. Shakiba, A. A novel randomized bit-level two-dimensional hyperchaotic image encryption algorithm. *Multimed. Tools Appl.* **2020**. [CrossRef]
41. Escobar, M.; Castillon, M.; Gutierrez, R.; Hernandez, C. Suggested Integral Analysis for Chaos-Based Image Cryptosystems. *Entropy* **2019**, *21*, 815. [CrossRef]
42. Ahmad, M.; Shamsi, U.; Khan, I. An enhanced image encryption algorithm using fractional chaotic systems. *Procedia Comput. Sci.* **2015**, *57*, 852–859. [CrossRef]
43. Rukhin, A.; Soto, J.; Nechvatal, J.; Smid, M.; Barker, E. A statistical test suite for random and pseudorandom number generators for cryptographic applications. NIST Special Publication 800-822 2001. Available online: http://www.nist.gov/manuscript-publication-search.cfm?pub_id=151222 (accessed on 15 May 2001).